Advanced Pharmaceutical Bulletin

Accepted Manuscript (unedited)

The manuscript will undergo copyediting, typesetting, and review of the resulting proof before it is published in its final form.

Research Article

How to cite this article:
Aprianti I, Iskandarsyah, Setiawan H. Transethosomal Diflunisal Gel: Physicochemical Characterization, Skin Permeation, and Antinociceptive Activity in Mice. Advanced Pharmaceutical Bulletin, doi: 10.34172/apb.47449

Transethosomal Diflunisal Gel: Physicochemical Characterization, Skin Permeation, and Antinociceptive Activity in Mice

Indah Aprianti[1*], Iskandarsyah[2], Heri Setiawan[3]

[1]Department of Pharmaceutical Technology, Faculty of Medicine, Universitas Tanjungpura, Pontianak, 78124, West Kalimantan, Indonesia.
[2]Faculty of Pharmacy Universitas Indonesia, Depok-16424, West Java, Indonesia
[3]Faculty of Pharmacy, Universitas Indonesia, Cluster of Health Sciences Building, Depok-16424, West Java, Indonesia

ARTICLE INFO

Keywords:
Antinociception;
Diflunisal;
Formalin test;
Skin permeation;
Transethosomes

Article History:
Submitted: June 01, 2026
Revised: July 19, 2026
Accepted: August 14, 2026
ePublished: August 31, 2026

ABSTRACT

Purpose: Diflunisal is a nonsteroidal anti-inflammatory drug whose topical delivery is constrained by low aqueous solubility and the stratum corneum barrier. This study characterized a diflunisal-loaded transethosomal gel and evaluated its ex vivo skin permeation, antinociceptive activity, and short-term physicochemical changes during storage.
Method: Diflunisal-loaded transethosomal gel was evaluated for physicochemical properties, ex vivo skin permeation, antinociceptive activity in Swiss mice (n = 8/group), and physicochemical changes during 12 weeks of storage. Permeation profiles were analyzed using a linear mixed-effects model, whereas flux and antinociceptive data were analyzed using one-way analysis of variance.
Results: Ex vivo permeation across excised mice skin demonstrated superior delivery from the transethosomal gel, with a cumulative permeation (Q) of 279.789 ± 6.351 µg/cm² compared with 177.688 ± 9.173 µg/cm² for the non-transethosomal gel. In vivo evaluation using the formalin-induced nociception model demonstrated significant antinociceptive activity in both phases. Formalin-evoked licking/biting times were lower in both diflunisal-treated groups than in the untreated formalin group. No statistically significant difference was observed between the oral and topically treated groups in this small experiment; this does not establish equivalence between the routes. Storage at 40 ± 2 °C produced greater changes in color, pH, viscosity, and measured drug content than storage at 30 ± 2 °C.
Conclusion: The diflunisal-loaded transethosomal gel enhanced ex vivo skin permeation and was associated with reduced formalin-evoked nociceptive behavior. These findings support further investigation of the formulation as a topical delivery system for diflunisal. Further pharmacokinetic, safety, vehicle-controlled, and disease-specific studies are required.

***Corresponding Author**
Indah Aprianti, Email: indahaprianti@pharm.untan.ac.id, ORCID: 0009-0000-0850-8480

Introduction

Non-steroidal anti-inflammatory drugs (NSAIDs) are widely used to manage inflammatory and musculoskeletal pain because they inhibit cyclooxygenase enzymes, thereby reducing prostaglandin-mediated inflammation and nociception.[1,2] Diflunisal, a salicylic acid derivative, possesses potent analgesic and anti-inflammatory activity and is used in the treatment of painful musculoskeletal conditions.[3–5] However, conventional oral administration of diflunisal is limited by intrinsic factors: low aqueous solubility, undesirable pharmacokinetic characteristics, and poor biodistribution. These pharmacokinetic challenges reduce bioavailability and therapeutic consistency, often necessitating higher doses that increase the risk of serious systemic adverse effects such as gastrointestinal ulceration, renal dysfunction, and cardiovascular events, particularly in elderly patients.[6,7]

To circumvent systemic toxicity and improve localized pain control, alternative delivery strategies have been explored. Topical and transdermal systems offer non-invasive routes for delivering drugs directly to peripheral tissues, bypassing hepatic first-pass metabolism and reducing systemic drug exposure.[8,9] Nevertheless, the stratum corneum, the outermost layer of the skin, poses a formidable barrier to drug penetration, especially for hydrophobic molecules like diflunisal. Conventional gel and cream formulations exhibit suboptimal permeation, resulting in inadequate therapeutic concentrations at target sites.[10]

Advanced vesicular carriers have emerged as promising platforms for enhancing transdermal drug delivery. Among these, ultra-deformable lipid systems such as ethosomes and transfersomes have demonstrated improved skin permeation by enhancing lipid bilayer fluidity and facilitating passage through intercellular lipid regions.[11] However, traditional ethosomal and transfersomal systems still face challenges in maximizing both drug loading and permeation efficiency concurrently, often requiring complex optimization that can compromise formulation stability or scalability.[12,13] Transethosomes, hybrid vesicular systems combining ethanol, phospholipids, and edge activators, represent a next-generation delivery platform that integrates the permeation enhancement mechanisms of both ethosomes and transfersomes. The synergy between ethanol's skin-fluidizing effect and edge activators' vesicle deformability results in substantially improved drug permeation across the stratum corneum. Transethosomes have been successfully employed to increase the transdermal delivery of various pharmacological agents, including peptides, analgesics, and anti-inflammatory drugs, with evidence of enhanced skin retention and controlled release kinetics.[14–17]

Despite these advances, the transethosomal delivery of diflunisal remains insufficiently characterized, particularly through an integrated assessment of vesicle properties, ex vivo skin permeation, short-term physicochemical stability, and in vivo antinociceptive activity. Previous studies have investigated diflunisal nanoparticles or ethosomal formulations; however, evidence directly linking the physicochemical performance of diflunisal-loaded vesicles with their biological activity remains limited. Therefore, the present study aimed to characterize a selected diflunisal-loaded transethosomal gel, compare its ex vivo permeation across excised mice skin with that of a non-transethosomal diflunisal gel, evaluate its effects on formalin-evoked nociceptive behavior in mice, and assess short-term physicochemical changes during storage. The formalin test was used as a biphasic model of acute neurogenic and inflammatory nociception.

Materials and methods

Materials

Diflunisal was purchased from Sigma-Aldrich Pte. Ltd., Singapore, Singapore. Phosphatidylcholine (Phospholipon® 90G) was sourced from Lipoid GmbH, Ludwigshafen, Germany. Span 80 and triethanolamine were obtained from Croda Singapore Pte. Ltd., Singapore, Singapore. Ethanol, methanol, dichloromethane, acetonitrile, potassium dihydrogen phosphate, sodium hydroxide, and formalin were supplied by Merck KGaA, Darmstadt, Germany. Carbopol® 934 was obtained from Shree Chemicals, Mumbai, India. Distilled water was purchased from PT Brataco, Jakarta, Indonesia. Swiss strain mice were obtained from the Research Hub, Universitas Padjadjaran, Sumedang, Indonesia.

Formulation of Transethosomes

Transethosomes were prepared using the thin-film hydration method. The formulation composition was adopted from the authors' previously published optimization study and was not optimized de novo in the present work.[18] The current study used this previously selected composition as a fixed formulation. It generated a new, independent dataset comprising physicochemical characterization, TEM imaging, ex vivo permeation, formalin-evoked nociceptive responses, and short-term stability. None of these data were reported in the earlier publications. The components and their respective quantities used in the formulation are outlined in Table 1. Accurate amounts of diflunisal, Phospholipon 90G, and edge activators were mixed and dissolved in a solvent mixture of dichloromethane and methanol (7:3 v/v), with a total volume of 20 ml. The organic solvents were then evaporated using a rotary evaporator (HS-3005S-N, Hahn Shin Scientific Co., Bucheon, Republic of Korea) at 52°C under reduced pressure, forming a thin film. To hydrate the thin film, a mixture of ethanol and phosphate buffer (pH 7.4) in a 3:7 (v/v) ratio was added, and the suspension was agitated for 1 hour using glass beads. For size reduction, the transethosome suspension was sonicated at 30% amplitude for 5 minutes.

Table 1. Components used in the formulation of transethosomes

Components	Amount (% w/v)
Diflunisal	1
Phospholipon 90G	2.5
Span 80	0.75
Ethanol: Phosphate buffer (pH 7.4) 3:7 (v/v)	ad 10 mL

Determination of Particle Size, Polydispersity Index, and Zeta Potential

Particle size, polydispersity index (PDI), and zeta potential of the diflunisal-loaded transethosomes were characterized using dynamic light scattering (DLS) with a Zeta-Sizer instrument (Malvern Zetasizer Nano ZS, Malvern Panalytical Ltd., Malvern, UK) at 25 °C. Transethosome suspensions were diluted with sterile water for injection at a 1:10 ratio and subsequently vortexed for 1 minute to ensure homogeneity. Each measurement was performed in triplicate to ensure reproducibility and reliability of the data.[19]

UV-Visible Spectrophotometry

Diflunisal was quantified by a validated UV-visible spectrophotometry method at 252 nm.[20] A 100 µg/mL stock solution was prepared, and the absorption spectrum was scanned over 200–400 nm to determine the wavelength of maximum absorption. Calibration standards ranging from 4 to 13 µg/mL were subsequently

analyzed. Linear regression yielded the equation (y = 0.0565x + 0.0137), with a coefficient of determination R^2 of 0.9993. Accuracy was evaluated in triplicate at 80%, 100%, and 120% of the target concentration, yielding mean recoveries of 98.594%, 99.696%, and 99.604%, respectively. Precision assessed at the corresponding concentration levels produced relative standard deviations of 0.741%, 0.359%, and 0.260%. The limits of detection and quantification were 0.3177 and 0.9627 µg/mL, respectively. Method selectivity was confirmed by the absence of detectable blank absorbance at the analytical wavelength.

Apparent Entrapment Efficiency (%EE)

The total diflunisal content and the apparent entrapment efficiency of transethosome suspensions were sequentially evaluated.[21] Vesicles were first disrupted by adding methanol to 1 mL of the suspension to a final volume of 5 mL, followed by vortexing for 5 minutes to ensure complete disruption. The solution was then diluted 1,250-fold with methanol for quantification of total diflunisal using UV–Vis spectrophotometry. Apparent entrapment efficiency was assessed indirectly by centrifuging 1 mL of the suspension at 10,000 rpm for 60 minutes at 4 °C. The supernatant (0.1 mL) was collected, diluted 500-fold with PBS, and the free diflunisal concentration was measured at 252 nm using UV–Vis spectrophotometry. The value is conservatively reported as apparent entrapment efficiency, representing an operational estimate of diflunisal association with the vesicular system rather than definitive intravesicular localization. All analyses were performed in triplicate, and entrapment efficiency (%EE) was calculated using the formula:

$$\%\text{EE} = \frac{\text{Total diflunisal (mg)} - \text{Free diflunisal (mg)}}{\text{Total diflunisal (mg)}} \text{x } 100\%$$

Transmission Electron Microscopy

Transethosome morphology was examined by transmission electron microscopy (TEM). A drop of the suspension was diluted 1:100 with buffer, applied to a copper grid, and incubated at room temperature for 15 minutes. Samples were negatively stained with 1% phosphotungstic acid for 3 minutes and imaged under TEM at 160 kV. Data are expressed as the mean ± SD from three independently prepared batches (n = 3).[18]

Formulation of Transethosome Gel

Diflunisal-loaded transethosome suspensions were incorporated into a gel base composed of 1% Carbopol 934. Carbopol was dispersed in distilled water and homogenized at 1,000 rpm. The gel pH was adjusted to 5 using triethanolamine (TEA) to achieve gelation. Methylparaben, pre-dissolved in propylene glycol, was incorporated into the gel matrix. The transethosome vesicles were then gradually added while continuously homogenizing at 1,000 rpm to obtain a uniform transethosomal diflunisal gel. For comparison, a non-transethosomal diflunisal gel was prepared by dissolving diflunisal (1 mg/mL) in phosphate buffer, then following the same gel preparation protocol.[22]

Ex Vivo Permeation Study

Fresh abdominal skin was excised from clinically healthy 2-month-old male *Swiss* mice weighing 30–35 g following hair removal and euthanasia, cleaned of adhering subcutaneous tissue, hydrated in phosphate-buffered saline (PBS; pH 7.4) for 30 min at 4 °C, and mounted between the donor and receptor compartments of Franz diffusion cells with the stratum corneum facing the donor compartment and the dermal surface facing the receptor phase. The receptor compartment contained 15 mL of PBS (pH 7.4), was maintained at 37 ± 0.5 °C, and was continuously stirred at 300 rpm; the effective diffusion area was 2.0096 cm^2. Gel containing 600 µg of diflunisal

was applied to the epidermal surface. At this donor dose and receptor volume, the maximum theoretical receptor concentration is approximately 89-fold below the reported diflunisal solubility in PBS at pH 7.4 (3.56 mg/mL), supporting sink conditions.[20] Receptor samples (2.5 mL) were collected at 0.25, 0.5, 1, 2, 3, 4, 5, 6, 8, 10, 12, 16, 20, and 24 h, with each withdrawn volume immediately replaced by an equal volume of fresh PBS. Diflunisal concentrations were quantified by UV–Vis spectrophotometry at 252 nm, and the cumulative amount permeated per unit area at sampling time n was corrected for serial sample removal using:

$$Q = \frac{\{Cn.V + \sum_{i=1}^{n-1} C\,S)}{A}$$

where C_n is the receptor-phase concentration at time n, V is the receptor volume, S is the sampling volume, C_i represents the concentrations measured in all preceding samples, and Ais the effective diffusion area. Cumulative permeation (μg/cm²) was plotted against time, and the steady-state flux (J, μg/cm²·h) was calculated from the slope of the linear portion of the permeation profile.[23,24] The study was designed to compare receptor-phase appearance and estimated flux between formulations under identical diffusion-cell conditions. Drug retained in the skin, remaining in the donor compartment, and recovered in wash fractions was not quantified; therefore, total mass balance was not established.

In Vivo Antinociceptive Study

All animal procedures were approved by the Health Research Ethics Committee of the Faculty of Medicine, Universitas Indonesia–Cipto Mangunkusumo Hospital (approval No. 1172/UN2.F1/ETIK/PPM.00.02/2022). A total of 33 physically healthy, 2-month-old male *Swiss* mice weighing 30–35 g were used: 9 in the preliminary formalin-concentration study and 24 in the main experiment. Male mice were selected to reduce variability associated with estrous-cycle hormonal fluctuations; this sex restriction limits generalizability to female animals. Mice were housed at up to five animals per cage, provided food and water ad libitum, maintained under a controlled 12-h light/12-h dark cycle, and acclimatized for 2 weeks before experimentation.

A preliminary study was conducted to determine the optimal formalin concentration for inducing a nociceptive response. Three groups of animals (n = 3 per group) were used: a control group receiving 0.9% NaCl, and two treatment groups receiving 2% and 2.5% formalin, respectively. Mice were individually placed in transparent acrylic observation chambers (13 × 13 × 10 cm), and nociceptive behaviors, such as licking and biting of the injected paw, were recorded during two phases: Phase I (0–5 min post-injection) and Phase II (20–30 min post-injection). The formalin concentration that elicited clear hyperalgesic behavior was selected for subsequent antinociceptive testing.

Table 2. Treatments for the antinociceptive study (n=8)

Group	Treatment
Negative Control	Formalin induction only
Treatment 1	Oral diflunisal (10mg/kg body weight) + formalin induction
Treatment 2	Transethosomal diflunisal gel (10mg/kg body weight) + formalin induction

For the antinociceptive study, mice were divided into three groups (n = 8 per group), as summarized in Table 2. Sample size was determined using the resource-equation approach for a one-way ANOVA design. For

three experimental groups, an error degrees of freedom range of 10–20 corresponds to 5–7 animals per group. Eight mice were included in each group, resulting in a degrees of freedom error of 21. Formalin was injected subplantarly (20 µL) into the right hind paw 1 hour after treatment administration. Mice received either oral or transdermal diflunisal at an effective dose of 10 mg/kg body weight, based on prior studies demonstrating analgesic and anti-inflammatory efficacy. Transethosomal gel was applied to shaved dorsal skin (2 × 2 cm) using a Finn chamber secured with an adhesive dressing, as seen in Figure 1, while oral formulations were administered via gavage. Nociceptive responses were recorded in the same acrylic chambers, with the duration of paw licking and biting measured separately for Phase I (acute, non-inflammatory pain) and Phase II (inflammatory pain).[25,26]

The in vivo experiment was designed as an exploratory active-comparator proof-of-concept to compare the formulated topical product with an established oral diflunisal treatment. For this reason, the design prioritized an oral active comparator and did not include vehicle-gel or blank-transethosome groups. This choice permits comparison with the oral-treatment group but does not isolate the contribution of diflunisal from possible effects of the gel base, ethanol, surfactant, phospholipid, occlusion, or handling. The 10 mg/kg topical value represents the nominal applied dose and was selected to match the administered oral dose pragmatically; it was not an exposure-matched comparison. Plasma or tissue pharmacokinetics, absorbed-dose recovery, residual topical drug, and validated dose-normalized exposure were not measured. Consequently, route equivalence, relative bioavailability, and component-specific efficacy cannot be concluded.

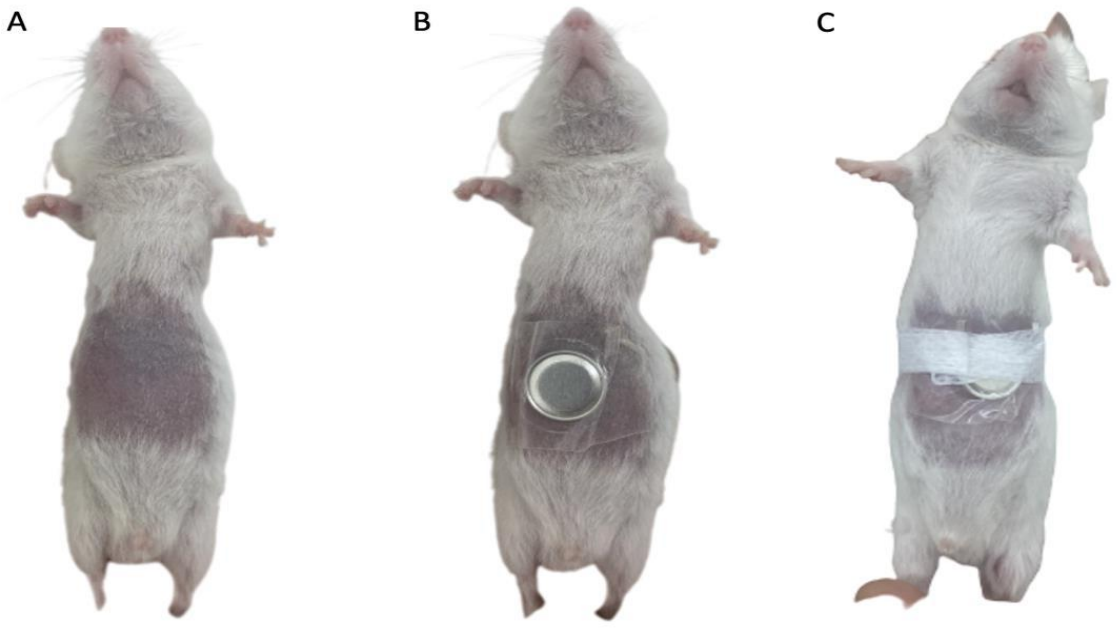

Figure 1. Gel application. Mice dorsal skin after shaving (A), placement of the gel using a Finn Chamber (B), adhesion of the gel and Finn Chamber (C).

Short-Term Storage Stability

Transethosomal gel, non-transethosomal diflunisal gel, and gel base were observed for 12 weeks at 30 ± 2 °C and 40 ± 2 °C, with assessments every 2 weeks. Recorded variables included appearance, homogeneity, viscosity, pH, and UV-visible absorbance-based drug content. The experiment was an exploratory short-term storage study and was not a formal shelf-life or ICH stability program.

Statistical Analysis

Data were analyzed using IBM SPSS Statistics version 24. *Ex vivo* permeation profiles were evaluated using a linear mixed-effects model with formulation, time, and their interaction as fixed effects. Flux data were analyzed using one-way ANOVA. Stability data were summarized descriptively because replicate-level observations were unavailable. Statistical significance was set at $p < 0.05$.

Results and discussion

Vesicle Size, PDI, and Zeta Potential

The thin-film hydration technique was employed for vesicle preparation, wherein a thin lipid film is first formed on the flask wall and subsequently hydrated with a hydroethanolic solvent [27]. This method was selected for its operational simplicity and for consistently yielding vesicles with optimal physicochemical characteristics, including particle size, polydispersity index (PDI), zeta potential, and high drug entrapment efficiency.[28]

Optimized diflunisal-loaded transethosomes displayed an average particle size of 78.23 ± 1.75 nm, a PDI of 0.283 ± 0.01, and a zeta potential of –31.83 ± 0.31 mV (Table 3). Nanoscale vesicles facilitate enhanced skin penetration, as sizes below 100 nm promote traversal through the stratum corneum and deposition in deeper dermal layers, which is critical for topical NSAID efficacy. Similar studies have reported that particle size in transethosomal formulations of lipophilic drugs, such as baicalin and curcumin, is correlated with improved *ex vivo* permeation and therapeutic outcomes.[29,30] The reduced vesicle size can be attributed to two key factors. First, high surfactant concentrations coat the vesicle surface, lowering interfacial tension and thereby producing smaller vesicles.[31] Second, ethanol incorporated into the transethosomal system further reduces particle size by inducing interpenetration of lipid hydrocarbon chains, resulting in more compact vesicular structures.[32,33]

A PDI value of 0.283 reflects a uniform vesicle population, ensuring predictable permeation and consistent release profiles. The literature indicates that transethosomal systems with PDI <0.3 exhibit stable, reproducible skin penetration, whereas higher PDI values are often associated with irregular drug delivery.[34]

Surface charge plays a dual role, influencing both physical stability and interactions with the negatively charged skin surface. The zeta potential of –31.83 mV observed in this study falls within the range commonly associated with kinetically stable vesicles and aligns with numerous lipid-based carriers reported in the literature. This negative charge is primarily attributed to the high ethanol content in the transethosomal formulation. Ethanol interacts with the polar head groups of phospholipids, imparting a negative charge that, in turn, generates electrostatic repulsion.[35] Negative surface charge may also facilitate repulsion from the stratum corneum lipid domains, reducing vesicle aggregation at the skin surface and favoring deeper penetration. In contrast, neutrally or weakly charged vesicles often exhibit greater coalescence tendencies, lowering permeation efficiency and supporting reliable performance in topical applications.[36,37]

Table 3. Physicochemical Characteristics of Diflunisal-Loaded Transethosomes. Results are expressed as mean ± SD (n = 3)

Parameter	Value
Particle size (nm)	78.23 ± 1.75
PDI	0.283 ± 0.01
Zeta potential (mV)	-31.83 ± 0.31
Apparent Entrapment Efficiency	78.68 ± 1.23

Apparent Entrapment Efficiency

Diflunisal-loaded transethosomes showed an apparent entrapment efficiency of 78.68 ± 1.23 % (Table 3), indicating that a substantial proportion of diflunisal was associated with the vesicular fraction under the applied separation conditions. This association may be related to the lipophilic nature of diflunisal, which favors partitioning into the hydrophobic regions of the phospholipid bilayer.[38,39] However, the analytical procedure did not distinguish drug incorporated within the vesicles from drug adsorbed onto vesicle surfaces or otherwise retained in the separated vesicular fraction. Accordingly, the value should be interpreted as an operational estimate of vesicle-associated diflunisal rather than definitive evidence of intravesicular encapsulation.

Transmission Electron Microscopy

Negative-stain TEM showed a heterogeneous population of closely packed, approximately spherical vesicular structures (Figure 2A). Some structures displayed internal electron-lucent regions or concentric contrast patterns that may be compatible with multilamellar or multivesicular organization; however, these features are not diagnostic of multivesicular vesicles. Negative-stain TEM provides a two-dimensional projection of stained and dehydrated specimens, and the apparent morphology may therefore be influenced by specimen preparation and stain-related contrast. Accordingly, the present image supports the formation of vesicular structures but does not establish multivesicular architecture. Confirmation would require cryogenic TEM across multiple representative fields, preferably complemented by electron tomography or another three-dimensional structural method. Cryogenic TEM preserves vesicles in a near-native hydrated state, while tomography can provide structural information that may not be resolved from individual two-dimensional projections.[40]

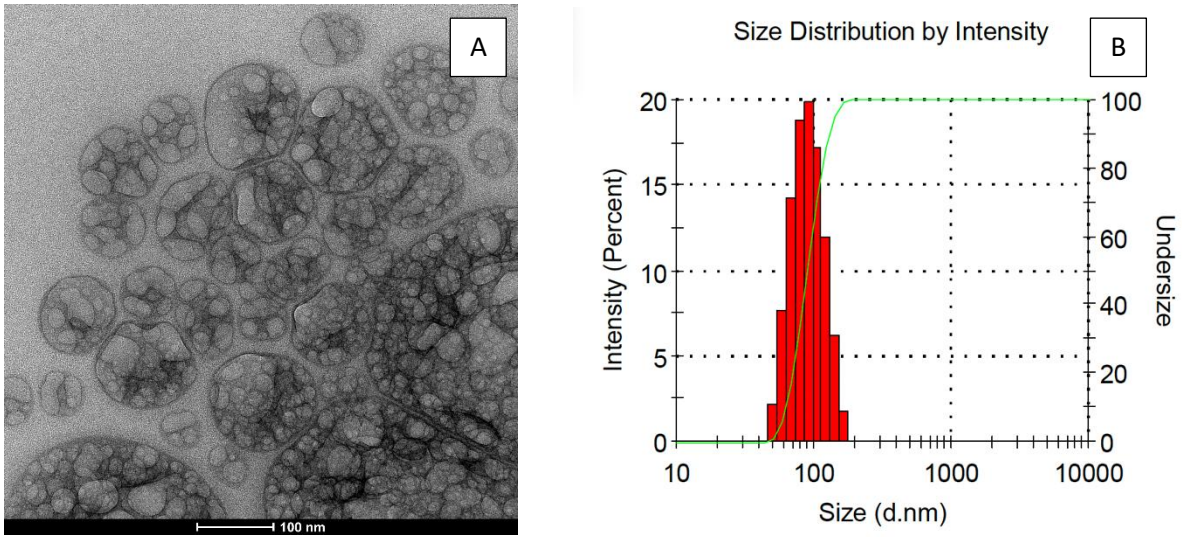

Figure 2. TEM Image (A) and Particle Size Distribution (B)

The observed internal contrast may nevertheless be considered in the context of previous reports showing that ethanol, phospholipid concentration, and preparation conditions can influence membrane curvature, lipid packing, and vesicle lamellarity in transethosomal systems. Ethanol increases bilayer fluidity and may promote structural heterogeneity, while phosphatidylcholine concentration and thin-film hydration conditions may affect vesicle organization and morphology. [35–38] These mechanisms provide a plausible explanation for the internal patterns observed in Figure 2A, but do not confirm multivesicular architecture in the present formulation. Similarly, potential functional consequences commonly associated with multilamellar or multivesicular systems,

such as enhanced drug retention or modified release, cannot be inferred from TEM images alone and require dedicated structural and release studies.

The dimensions observed by TEM were broadly within the nanoscale range but were not considered directly equivalent to the DLS results (Figure 2B). DLS derives an equivalent hydrodynamic diameter from the translational diffusion of particles in dispersion, whereas TEM provides projected dimensions of the structures visualized after specimen preparation. In addition, intensity-weighted DLS distributions are disproportionately influenced by larger particles or aggregates. Therefore, DLS and TEM should be interpreted as complementary measurements of distinct physical properties rather than as direct confirmation of each other. Quantitative comparison would require image-based measurement of a sufficiently large and representative particle population and comparison with the appropriate DLS size-distribution metric.[41]

Ex Vivo Permeation Study

Ex vivo skin permeation was evaluated using a Franz diffusion cell, a widely accepted model for assessing transdermal drug transport. In this system, excised skin was mounted between the donor and receptor compartments to monitor drug diffusion across the skin over time and to determine the cumulative amount permeated per unit area (Q) and flux (J).[42] PBS pH 7.4 was used as the receptor medium without additional surfactants or solubilizers, as diflunisal showed sufficient solubility in this medium (3.56 mg/mL),[20] which was substantially higher than the total amount of drug applied in the donor compartment (600 μg). This confirmed that the study was conducted under sink conditions throughout the experiment, ensuring that the permeation profile reflected the formulation's intrinsic performance rather than being limited by drug solubility.[43]

The permeation study, conducted at 14 sampling points, revealed a clear superiority of the transethosomal gel over the non-transethosomal gel in promoting diflunisal transport across the skin. As presented in Figure 3A, the cumulative amount of diflunisal permeated from the transethosomal gel containing Span 80 at 0.75% reached 279.789 ± 6.351 μg/cm². In contrast, the non-transethosomal diflunisal gel exhibited a substantially lower cumulative permeation of 177.688 ± 9.173 μg/cm². Cumulative permeation differed significantly over time, $F(13, 40.419) = 157.624$, $p < 0.001$, and between the two formulations, $F(1, 5.396) = 455.731$, $p < 0.001$. A significant formulation-by-time interaction was also observed, $F(13, 40.419) = 20.310$, $p < 0.001$, indicating that the magnitude of the difference between the transethosomal and non-transethosomal gels varied throughout the 24-hour study period. This marked difference demonstrates that incorporation of diflunisal into the transethosomal vesicular system significantly improved its ability to traverse the skin barrier.

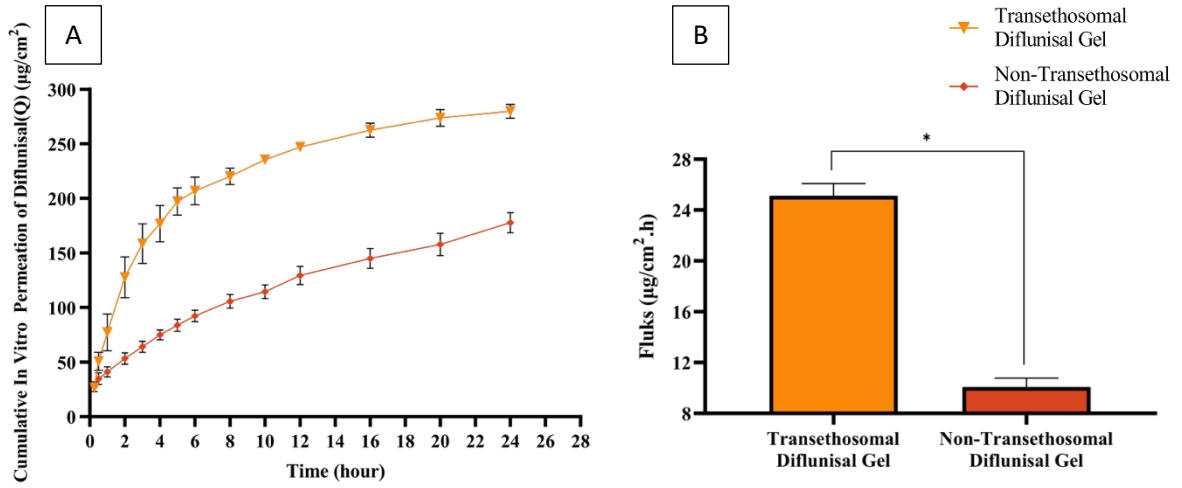

Figure 3. *Ex vivo* permeation of transethosomal and non-transethosomal diflunisal gels: (A) cumulative amount permeated (µg/cm²) and (B) flux (µg/cm²·h). Data are presented as mean ± SD (n = 3). *p < 0.05.

The relatively low permeation observed for the non-transethosomal gel is most plausibly attributable to the intrinsic physicochemical properties of diflunisal. Diflunisal is a lipophilic drug with a log P value of 4.44,[44] and although lipophilicity generally favors partitioning into the stratum corneum, transdermal permeation is not linearly improved by increasing lipophilicity. Rather, skin permeability is known to follow a parabolic relationship with lipophilicity, with maximal permeation typically occurring at a log P of approximately 3-4.[45] Therefore, the lipophilicity of diflunisal, being slightly above the optimal range, may promote retention within the lipid-rich stratum corneum while limiting its onward diffusion into the deeper, more aqueous epidermal and dermal layers.[46] In the absence of a specialized carrier system, this physicochemical constraint results in suboptimal permeation, as reflected by the lower cumulative amount penetrated observed for the conventional gel. By contrast, the higher amount of diflunisal permeated from the transethosomal gel can be attributed to the synergistic interplay among the vesicular components and the unique biophysical behavior of the transethosomal system.[17]

Another key parameter for interpreting permeation performance is flux, which represents the rate of drug transport across the membrane per unit area per unit time and is calculated from the slope of the linear portion of the cumulative permeation-time profile according to Fick's first law of diffusion. Flux, therefore, reflects the efficiency with which a formulation can sustain drug movement through the skin under quasi-steady-state conditions. As presented in Figure 3B, the transethosomal gel exhibited a flux of 25.129 ± 0.958 µg/cm²·h, which was substantially higher than that of the non-transethosomal gel (10.074 ± 0.698 µg/cm²·h), and this difference was statistically significant ($p < 0.05$). This finding confirms that the transethosomal system not only increased the total amount of diflunisal delivered across the skin but also substantially accelerated the rate of permeation.

The superior permeation and flux of the transethosomal gel are attributed to the synergistic effect of the vesicular components and the unique structural characteristics of the transethosomal system.[17] Span 80 acts as an edge activator that increases vesicle deformability by reducing the rigidity of the lipid bilayer, thereby enabling the vesicles to pass through narrow intercellular pathways within the stratum corneum.[14,47] Ethanol also plays a critical role as a penetration enhancer by interacting with skin lipids, disturbing their ordered packing, and increasing membrane fluidity. In addition, phospholipids together with ethanol can loosen the intercellular lipid structure of the stratum corneum and improve drug partitioning into the skin. Ethanol and surfactants are also

known to reduce the phase transition temperature of skin lipids by intercalation into lipid bilayers, thereby increasing lipid fluidity and decreasing diffusional resistance.[48] Collectively, these effects facilitate deeper skin penetration and more efficient transport of diflunisal, which explains the markedly higher cumulative permeation and flux observed for the transethosomal gel compared with the non-transethosomal gel.

Overall, the *ex vivo* permeation data unequivocally demonstrate the advantage of the transethosomal carrier system for the topical delivery of diflunisal. The significantly higher cumulative amount permeated and the markedly greater flux indicate that transethosomes successfully overcame the permeation limitations associated with the high lipophilicity of diflunisal. From a formulation perspective, these findings highlight the ability of the transethosomal system to combine penetration enhancement, vesicle deformability, and favorable drug-skin partitioning into a single delivery platform. From a therapeutic standpoint, the enhanced permeation profile suggests that transethosomal gel may offer superior potential for achieving effective local drug levels in the skin and underlying tissues, thereby supporting its further development as an advanced topical delivery system for diflunisal in pain management applications. Interpretation remains limited by the absence of skin-retention, donor-recovery, wash-fraction, and total mass-balance measurements. Mice skin is generally more permeable than human skin; therefore, the magnitude of permeation should not be directly extrapolated to clinical performance. Human or porcine skin with complete mass-balance assessment would provide a more informative barrier model for subsequent studies.

In Vivo Antinociceptive Study

Formalin-induced nociception was selected as an in vivo pain model because it enables simultaneous assessment of neurogenic and inflammatory components of pain within a single assay. Phase I (0–5 min) reflects acute nociception caused by direct activation of peripheral C-fibers, whereas Phase II (20–30 min) represents inflammatory pain associated with peripheral mediator release and central sensitization.[49–51] Such a biphasic response makes this model particularly relevant for diflunisal, an NSAID whose analgesic efficacy is closely linked to inflammation-driven nociception.

Preliminary evaluation demonstrated that both 2% and 2.5% formalin induced significant nociceptive responses in both phases compared with 0.9% NaCl ($p < 0.05$) as seen in Figure 4A. Formalin at 2.5% produced a significantly greater response in Phase I and a numerically higher, but non-significant, response in Phase II than formalin 2%. Comparable observations have been reported previously, indicating that increasing formalin concentration mainly intensifies the early neurogenic component without substantially enhancing the late inflammatory phase.[52] Because the pilot was not powered for confirmatory statistical inference or formal concentration optimization, statistical comparisons were not used to establish the superiority of either concentration. Before the main experiment, 2% formalin was selected prospectively as the lowest concentration to elicit a clear biphasic response and an adequate Phase II signal, while avoiding the stronger early-phase irritant stimulus observed with 2.5% formalin. This selection was therefore exploratory and pragmatic and should not be interpreted as evidence that 2% formalin was statistically optimal.

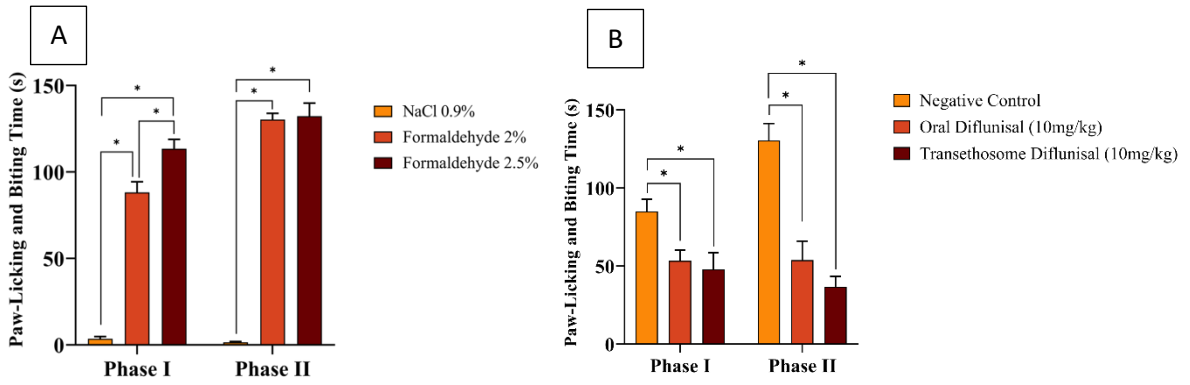

Figure 4. In vivo antinociceptive activity in mice: (A) nociceptive responses to different formalin concentrations (n = 3) and (B) treatment effects on formalin-induced pain (n = 8). Data are presented as mean ± SD. *p < 0.05.

Robust antinociceptive activity was observed for both oral diflunisal and diflunisal-loaded transethosomal gel, as shown in Figure 4B. During Phase I, licking and biting time decreased significantly ($p < 0.05$) from 79.664 ± 11.917 s in the negative control group to 49.495 ± 9.307 s in the oral group and 46.731 ± 9.948 s in the transdermal group, corresponding to reductions of 37.87% and 41.34%, respectively. More pronounced inhibition was observed in Phase II, where nociceptive time declined from 120.963 ± 20.586 s in the negative control to 48.336 ± 16.846 s after oral administration and 44.090 ± 22.829 s after transdermal treatment, corresponding to 60.04% and 63.55% inhibition, respectively. The absence of a significant difference between oral and transdermal diflunisal in either phase ($p > 0.05$) indicates comparable in vivo efficacy between the two delivery routes.

Preferential inhibition during Phase II is mechanistically consistent with the pharmacological action of diflunisal. This study aligns with the findings of Kaur et al. (2017) and Sallam et al. (2013), which showed that transdermal diflunisal formulations reduced pain in both phases I and II of the formalin test, with a notably stronger effect in Phase II [20,53]. Diflunisal inhibits COX-1 and COX-2, thereby suppressing prostaglandin synthesis and reducing nociceptor inflammatory sensitization. These enzymes convert arachidonic acid into inflammatory mediators, such as prostaglandins. Inhibition of COX enzymes reduces prostaglandin synthesis, which plays a crucial role in the inflammatory and pain pathways. The analgesic action of NSAIDs, such as diflunisal, stems from decreased prostaglandin synthesis in peripheral tissues and the central nervous system. While prostaglandins themselves do not directly cause pain, they sensitize peripheral nociceptors to mediators like bradykinin and histamine.[54]

Comparable activity between oral diflunisal and transethosomal gel further suggests that transethosomal delivery provided sufficient skin penetration to achieve a pharmacologically meaningful antinociceptive response. However, because vehicle-gel and blank-transethosome-gel groups were not included, the observed response cannot be attributed specifically to diflunisal. Possible contributions from ethanol, surfactant, phospholipid, the gel base, occlusion, and handling cannot be excluded. Moreover, although no statistically significant difference was detected between the oral and topical diflunisal groups, the study was not designed or powered as an equivalence or non-inferiority trial. Therefore, the findings do not establish comparable efficacy between the two administration routes. Previous studies have suggested that ethosomal systems may enhance the dermal delivery of NSAIDs.[55] However, this mechanism was not directly demonstrated in the present study because skin deposition, local exposure, and systemic exposure were not quantified. Accordingly, the results should be interpreted as preliminary evidence of the antinociceptive activity of the tested diflunisal-loaded transethosomal formulation.

Short-Term Storage Stability

Short-term storage stability demonstrated that storage temperature markedly influenced the physical and chemical integrity of the gel systems. During 12 weeks of storage at 30 ± 2 °C, transethosomal gel, non-transethosomal gel, and gel base retained their original organoleptic characteristics, with no detectable change in color, odor, or homogeneity. Transethosomal gel remained white with a characteristic odor, whereas non-transethosomal gel remained colorless and odorless, and gel base remained colorless with the characteristic odor of Carbopol. In contrast, accelerated storage at 40 ± 2 °C induced visible discoloration in the transethosomal gel from week 8 onward, progressing from white to yellowish white and eventually to pale yellow at week 12, while the non-transethosomal gel and gel base remained visually unchanged. Such selective discoloration strongly suggests reduced stability of the phospholipid-based vesicular system under thermal stress. Phosphatidylcholine is known to undergo hydrolytic degradation in the presence of heat and moisture, generating lysophosphatidylcholine and free fatty acids, which may contribute to both color alteration and overall physicochemical instability.[56]

Rheological analysis (Figure 5A, 5B) further confirmed temperature-dependent instability. Viscosity progressively decreased in both gel formulations over the storage period at 30 ± 2 °C and 40 ± 2 °C, with a more pronounced decline under accelerated conditions. Such behavior is consistent with the pH-dependent nature of Carbopol gels, whose viscosity is maintained by ionization and expansion of the polymeric network. Progressive acidification of the formulations would therefore reduce polymer swelling and compromise gel structure, leading to lower viscosity.[57]

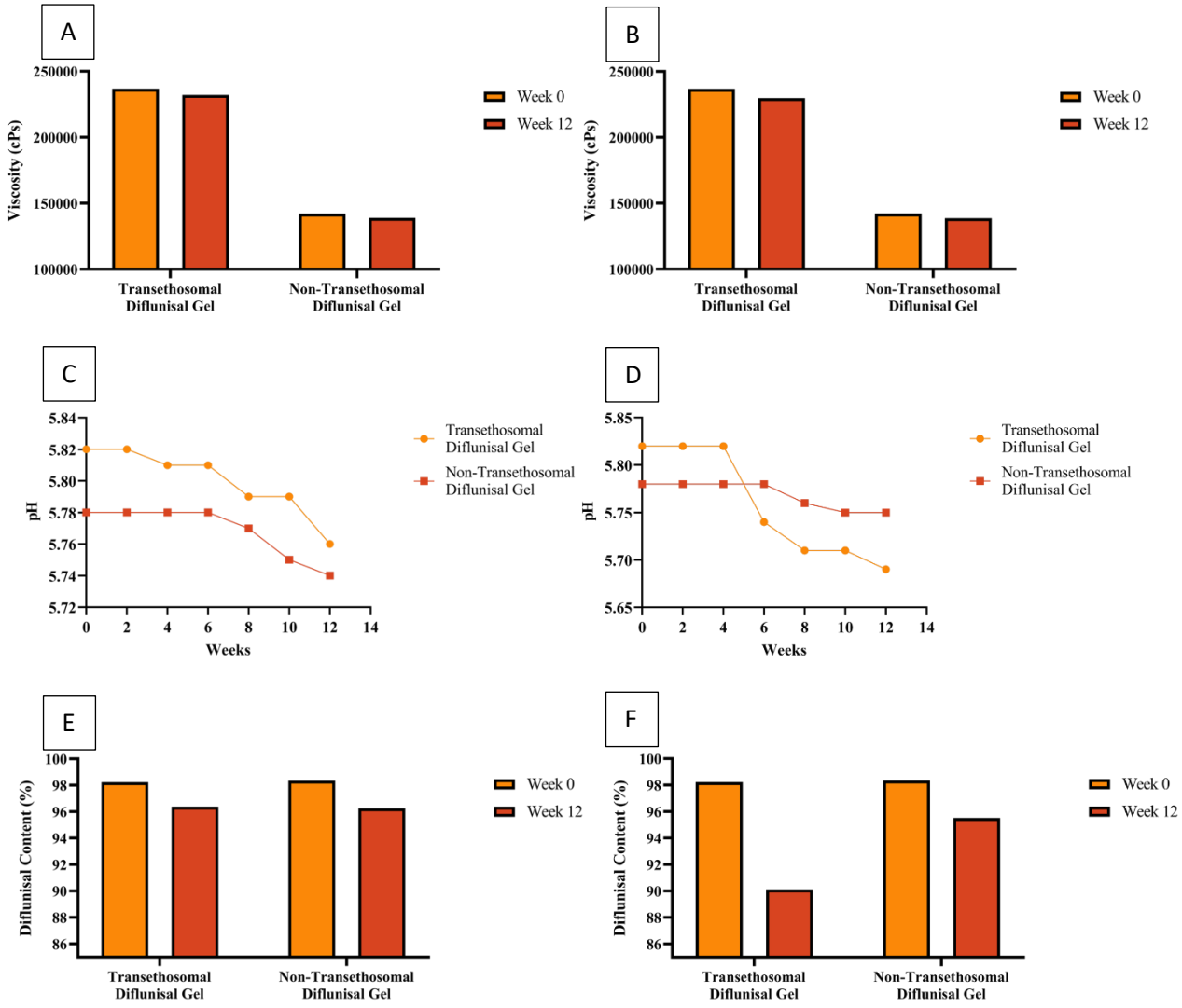

Figure 5. Short-term storage stability profiles of transethosomal and non-transethosomal diflunisal gels during 12 weeks of storage: viscosity at (A) 30 ± 2 °C and (B) 40 ± 2 °C; pH at (C) 30 ± 2 °C and (D) 40 ± 2 °C; and drug content at (E) 30 ± 2 °C and (F) 40 ± 2 °C.

pH monitoring revealed a gradual decline in both formulations during storage; however, all values remained within the physiologically acceptable skin pH range of 4.5–6.5 (Figure 5C, 5D). Most pronounced acidification occurred in the transethosomal gel stored at 40 ± 2 °C, in agreement with the greater color instability observed under the same condition. Such findings support the occurrence of phospholipid degradation during storage, particularly in the transethosomal system, where formation of free fatty acids could account for the shift toward a more acidic environment.[58]

Drug content analysis showed a gradual reduction in diflunisal concentration in both formulations during storage, with the greatest loss observed in the transethosomal gel under accelerated conditions (Figure 5E, 5F). This pattern was fully consistent with the physical and chemical changes observed in the same formulation, namely discoloration, a decline in pH, and a reduction in viscosity. Taken together, these results indicate that diflunisal-loaded transethosomal gel remained acceptably stable at 30 ± 2 °C for up to 3 months. In contrast, elevated temperatures accelerated degradation of the vesicular system and compromised formulation stability. Such findings underscore the importance of controlled storage conditions for preserving the performance of phospholipid-based transdermal delivery systems.

Taken together, short-term stability data suggest that the transethosomal gel remained sufficiently stable at 30 ± 2 °C throughout the 12-week study period. More pronounced changes under accelerated conditions suggest that elevated temperature may promote the degradation of vesicular phospholipids and adversely affect the formulation's physicochemical characteristics. These findings are exploratory and do not establish shelf life, room-temperature stability, or an appropriate commercial storage condition.

Conclusion

Under the tested conditions, the diflunisal-loaded transethosomal gel increased receptor-phase permeation across excised mice skin relative to the non-transethosomal diflunisal gel and was associated with reduced formalin-evoked nociceptive behavior in mice. Physicochemical changes during 12 weeks of storage were less pronounced at 30 ± 2 °C than at 40 ± 2 °C. These findings support further evaluation of the formulation but do not establish efficacy in osteoarthritis, superior safety, or equivalence to oral diflunisal. Further studies should incorporate appropriate pharmacokinetic and safety assessments, and disease-relevant pain models.

Ethical Approval

The animal study was approved by the Health Research Ethics Committee of the Faculty of Medicine, Universitas Indonesia–Cipto Mangunkusumo Hospital (approval No. 1172/UN2.F1/ETIK/PPM.00.02/2022).

Authors' Contribution

Conceptualization: Indah Aprianti, Iskandarsyah, Heri Setiawan
Data curation: Indah Aprianti, Iskandarsyah, Heri Setiawan
Formal analysis: Indah Aprianti
Funding acquisition: Indah Aprianti, Iskandarsyah, Heri Setiawan
Investigation: Indah Aprianti
Methodology: Indah Aprianti, Iskandarsyah, Heri Setiawan
Project administration: Indah Aprianti, Iskandarsyah, Heri Setiawan
Resources: Indah Aprianti, Iskandarsyah, Heri Setiawan
Software: Indah Aprianti
Supervision: Iskandarsyah, Heri Setiawan
Validation: Indah Aprianti, Iskandarsyah, Heri Setiawan
Visualization: Indah Aprianti
Writing–original draft: Indah Aprianti, Iskandarsyah, Heri Setiawan
Writing–review & editing: Indah Aprianti, Iskandarsyah, Heri Setiawan

Declaration of Conflicting Interests

The authors declare that there are no conflicts of interest regarding the publication of this article.

Declaration of generative AI and AI-assisted technologies in the manuscript preparation process

During preparation of this manuscript, the author used Grammarly and ChatGPT (OpenAI) solely for English-language editing and stylistic refinement. The author subsequently reviewed and revised all edited text and takes full responsibility for the accuracy, integrity, and final content of the article.

References

1. Arfeen M, Srivastava A, Srivastava N, Khan RA, Almahmoud SA, Mohammed HA. Design, classification, and adverse effects of NSAIDs: A review on recent advancements. Bioorg Med Chem. 2024;112:117899. doi:10.1016/j.bmc.2024.117899
2. Gunaydin C, Bilge SS. Effects of nonsteroidal anti-inflammatory drugs at the molecular level. Eurasian J Med. AVES İbrahim KARA; 2018. p. 116–21. doi:10.5152/eurasianjmed.2018.0010

3. Brogden RN, Heel RC, Pakes GE, Speight TM, Avery GS. Diflunisal: A Review of its Pharmacological Properties and Therapeutic Use in Pain and Musculoskeletal Strains and Sprains and Pain in Osteoarthritis. Drugs. 1980;19(2):84–106. doi:10.2165/00003495-198019020-00002
4. Hannah J, Ruyle W, Jones H, Matzuk A, Kelly K, Witzel B, et al. Discovery of diflunisal. Br J Clin Pharmacol. 1977;4(1 S):7S-13S. doi:10.1111/j.1365-2125.1977.tb04508.x PubMed PMID: 328036.
5. DiPiro JT, Yee GC, Haines ST, Nolin TD, Ellingrod VL, Posey M. DiPiro's Pharmacotherapy: A Pathophysiologic Approach. Twelfth Edition. McGraw Hill; 2023.
6. Snetkov P, Morozkina S, Olekhnovich R, Uspenskaya M. Diflunisal targeted delivery systems: A review. Materials. 2021 Nov 1;14(21). doi:10.3390/ma14216687
7. Maria Pacifici G. Clinical Pharmacology of Diflunisal. International Journal of Clinical Studies and Medical Case Reports. 2024 Oct 17;43(3). doi:10.46998/ijcmcr.2024.43.001065
8. Zhao L, Chen J, Bai B, Song G, Zhang J, Yu H, et al. Topical drug delivery strategies for enhancing drug effectiveness by skin barriers, drug delivery systems and individualized dosing. Frontiers in Pharmacology. 2023. doi:10.3389/fphar.2023.1333986
9. Karthikeyan E, Sivaneswari S. Advancements in transdermal drug delivery systems: Enhancing medicine with pain-free and controlled drug release. Intelligent Pharmacy. KeAi Publishing Communications Ltd.; 2025. p. 277–95. doi:10.1016/j.ipha.2024.09.008
10. Balmanno A, Falconer JR, Ravuri HG, Mills PC. Strategies to Improve the Transdermal Delivery of Poorly Water-Soluble Non-Steroidal Anti-Inflammatory Drugs. Pharmaceutics. 2024. doi:10.3390/pharmaceutics16050675
11. Erdoğar N, Gür B, Örgül D. Recent developments of novel nanotechnology-based drug delivery systems for dermal and transdermal applications. Eur J Pharm Sci. 2026. doi:10.1016/j.ejps.2025.107413 PubMed PMID: 41389911.
12. Almuqbil RM, Aldhubiab B. Ethosome-Based Transdermal Drug Delivery: Its Structural Components, Preparation Techniques, and Therapeutic Applications Across Metabolic, Chronic, and Oncological Conditions. Pharmaceutics. Multidisciplinary Digital Publishing Institute (MDPI); 2025. doi:10.3390/pharmaceutics17050583 PubMed PMID: 40430874.
13. Medhi J, Thalluri C, Vasam M, Bukke SPN. The future of vesicular drug delivery: transferosomes in therapeutic advancement—applications, innovations and challenges. BioMedical Engineering Online. BioMed Central Ltd; 2026. doi:10.1186/s12938-025-01490-6 PubMed PMID: 41331612.
14. Patra P. Cutting-edge advances in transethosomes and nanoethosomes for transdermal drug delivery. Discover Chemistry. 2025 Jun 19;2(1). doi:10.1007/s44371-025-00232-w
15. Ali J, Raza R, Ameen S, Arshad A, Karim F, Waseem Akram M, et al. Transethosomes: A Breakthrough System for Transdermal and Topical Drug Delivery. Pakistan BioMedical Journal. 2022 Jul 31. doi:10.54393/pbmj.v5i7.578
16. Bajaj KJ, Parab BS, Shidhaye SS. Nano-transethosomes: A novel tool for drug delivery through skin. Indian Journal of Pharmaceutical Education and Research. 2021 Jan 1;55(1):s1–10. doi:10.5530/ijper.55.1s.33
17. Kumar Mishra K, Deep Kaur C, Verma S, Kumar Sahu A, Kumar Dash D, Kashyap P, et al. Transethosomes and Nanoethosomes: Recent Approach on Transdermal Drug Delivery System. In: Farrukh MA, editor. Nanomedicines. London: IntechOpen; 2019. p. 13. doi:10.5772/intechopen.81152
18. Aprianti I, Iskandarsyah, Setiawan H. Diflunisal Transethosomes for Transdermal Delivery: Formulation and Characterization. International Journal of Applied Pharmaceutics. 2023 May 7;15(3):61–6. doi:10.22159/ijap.2023v15i3.47691

19. Ma N, Chen S, Miao J, Zhao R, Gao Q, Zhang M, et al. From Juanbi Qianggu formula to a self-assembled nanodrug: identifying macrophage repolarization candidates and developing a carrier-free system for enhanced anti-inflammatory efficacy. J Drug Deliv Sci Technol. 2026 Jun 1;120. doi:10.1016/j.jddst.2026.108183
20. Kaur A, Bhoop BS, Chhibber S, Sharma G, Gondil VS, Katare OP. Supramolecular nano-engineered lipidic carriers based on diflunisal-phospholipid complex for transdermal delivery: QbD based optimization, characterization and preclinical investigations for management of rheumatoid arthritis. Int J Pharm. 2017 Nov 25;533(1):206–24. doi:10.1016/j.ijpharm.2017.09.041 PubMed PMID: 28943207.
21. Fabiano MG, Maurizi L, Forte J, D'Intino E, Ammendolia MG, Corinti D, et al. A green strategy for resveratrol nanodelivery: A multidisciplinary approach for the physicochemical characterization of Thymus-based liposomes with anti-biofilm activity against Listeria monocytogenes. J Drug Deliv Sci Technol. 2026 Mar 1;117. doi:10.1016/j.jddst.2026.108027
22. Aprianti I, Pranata K, Hitri IZ. Diflunisal transethosomal gel for topical drug delivery: Formulation and Characterization. Medical Sains : Jurnal Ilmiah Kefarmasian. 2025;10(4):453–62. doi:10.37874/ms.v10i4.1846
23. Xiao Y, Zhou L, Tao W, Yang X, Li J, Wang R, et al. Preparation of paeoniflorin-glycyrrhizic acid complex transethosome gel and its preventive and therapeutic effects on melasma. European Journal of Pharmaceutical Sciences. 2024 Jan 1;192. doi:10.1016/j.ejps.2023.106664 PubMed PMID: 38061662.
24. Jaikham P, Leelapornpisid P, Tragoolpua K, Koonyosying P, Lin WC, Poomanee W. Transethosomes-encapsulated Bouea macrophylla seed extract for anti-acne application: Formulation optimization, antibacterial efficacy, and safety assessment. J Agric Food Res. 2025 Apr 1;20. doi:10.1016/j.jafr.2025.101764
25. Yaghooti P, Alimoahmmadi S. Assessment of antinociceptive property of Cynara scolymus L. and possible mechanism of action in the formalin and writhing models of nociception in mice. Korean J Pain. 2024;37(3):218–32. doi:10.3344/kjp.23355
26. Ortiz MI, Cariño-Cortés R, Fernández-Martínez E, Muñoz-Pérez VM, Castañeda-Hernández G, González-García MP. Peripheral Antinociception Induced by Carvacrol in the Formalin Test Involves the Opioid Receptor-NO-cGMP-K+ Channel Pathway. Metabolites. 2025 May 1;15(5). doi:10.3390/metabo15050314
27. Xiang B, Cao DY. Preparation of Drug Liposomes by Thin-Film Hydration and Homogenization. In. 2021. p. 25–35. doi:10.1007/978-3-662-49320-5_2
28. Dayal D, Kalra N. Comparative Evaluation of Thin Film Hydration vs. Reverse Phase Evaporation for Liposomal Drug Delivery Systems. Journal of Advances in Developmental Research [Internet]. 2026;17(1). Available from: www.ijaidr.com•
29. Rezigue M, Aljabali AAA, Alshaer W. Transethosome-mediated curcumin delivery promotes superior wound healing with reduced toxicity. Pharmacia. 2025;72. doi:10.3897/pharmacia.72.e161022
30. Adin SN, Gupta I, Aqil M, Mujeeb M. Baicalin loaded transethosomes for rheumatoid arthritis: Development, characterization, pharmacokinetic and pharmacodynamic evaluation. J Drug Deliv Sci Technol. 2023 Mar 1;81. doi:10.1016/j.jddst.2023.104209
31. Rasool M, Mazhar D, Afzal I, Zeb A, Khan S, Ali H. In vitro and in vivo characterization of Miconazole Nitrate loaded transethosomes for the treatment of Cutaneous Candidiasis. Int J Pharm. 2023 Nov 25;647. doi:10.1016/j.ijpharm.2023.123563 PubMed PMID: 37907141.
32. Jamshaid H, Din F ud, Nousheen K, Khan SU, Fatima A, Khan S, et al. Mannosylated imiquimod-terbinafine co-loaded transethosomes for cutaneous leishmaniasis; assessment of its anti-leishmanial potential, in vivo safety and immune response modulation. Biomaterials Advances. 2023 Feb 1;145. doi:10.1016/j.bioadv.2022.213266

33. El-Sonbaty MM, Akl MA, El-Say KM, Kassem AA. Does the technical methodology influence the quality attributes and the potential of skin permeation of Luliconazole loaded transethosomes? J Drug Deliv Sci Technol. 2022 Feb 1;68. doi:10.1016/j.jddst.2022.103096
34. Vera Pérez J, Martínez Cortés DM, Gómez y Gómez Y. Potential use of transethosomes as a transdermal delivery system for metabolites from Chenopodium murale. Mater Today Commun. 2022 Mar 1;30. doi:10.1016/j.mtcomm.2022.103165
35. Bin Jardan YA, Ahad A, Raish M, Al-Jenoobi FI. Preparation and Characterization of Transethosome Formulation for the Enhanced Delivery of Sinapic Acid. Pharmaceutics. 2023 Oct 1;15(10). doi:10.3390/pharmaceutics15102391
36. Li L, Wang H, Ye J, Chen Y, Wang R, Jin D, et al. Mechanism Study on Nanoparticle Negative Surface Charge Modification by Ascorbyl Palmitate and Its Improvement of Tumor Targeting Ability. Molecules. 2022 Jul 1;27(14). doi:10.3390/molecules27144408 PubMed PMID: 35889281.
37. Németh Z, Csóka I, Semnani Jazani R, Sipos B, Haspel H, Kozma G, et al. Quality by Design-Driven Zeta Potential Optimisation Study of Liposomes with Charge Imparting Membrane Additives. Pharmaceutics. 2022 Sep 1;14(9). doi:10.3390/pharmaceutics14091798
38. Jain SK, Gupta Y, Jain A, Bhola M. Multivesicular liposomes bearing celecoxib-β-cyclodextrin complex for transdermal delivery. Drug Deliv. 2007 Aug;14(6):327–35. doi:10.1080/10717540601098740 PubMed PMID: 17701522.
39. Sun Q, Liang J, Lin Y, Zhang Y, Yan F, Wu W. Preparation of nano-sized multi-vesicular vesicles (MVVs) and its application in co-delivery of doxorubicin and curcumin. Colloids Surf B Biointerfaces. 2023 Sep 1;229. doi:10.1016/j.colsurfb.2023.113471 PubMed PMID: 37523805.
40. Peretz Damari S, Shamrakov D, Varenik M, Koren E, Nativ-Roth E, Barenholz Y, et al. Practical aspects in size and morphology characterization of drug-loaded nano-liposomes. Int J Pharm. 2018;547(1):648–55. doi:10.1016/j.ijpharm.2018.06.037
41. Filippov SK, Khusnutdinov R, Murmiliuk A, Inam W, Zakharova LY, Zhang H, et al. Dynamic light scattering and transmission electron microscopy in drug delivery: a roadmap for correct characterization of nanoparticles and interpretation of results. Materials Horiz. Royal Society of Chemistry; 2023. p. 5354–70. doi:10.1039/d3mh00717k PubMed PMID: 37814922.
42. Kumar M, Sharma A, Mahmood S, Thakur A, Mirza MA, Bhatia A. Franz diffusion cell and its implication in skin permeation studies. J Dispers Sci Technol. 2023. doi:10.1080/01932691.2023.2188923
43. Abd El-Alim SH, Kassem AA, Basha M, Salama A. Comparative study of liposomes, ethosomes and transfersomes as carriers for enhancing the transdermal delivery of diflunisal: In vitro and in vivo evaluation. Int J Pharm. 2019 May 30;563:293–303. doi:10.1016/j.ijpharm.2019.04.001 PubMed PMID: 30951860.
44. National Center for Biotechnology Information. https://pubchem.ncbi.nlm.nih.gov/compound/Diflunisal. 2022. PubChem Compound Summary for CID 3059, Diflunisal.
45. Albash R, Abdelbary AA, Refai H, El-Nabarawi MA. Use of transethosomes for enhancing the transdermal delivery of olmesartan medoxomil: In vitro, ex vivo, and in vivo evaluation. Int J Nanomedicine. 2019;14:1953–68. doi:10.2147/IJN.S196771 PubMed PMID: 30936696.
46. Hmingthansanga V, Singh N, Banerjee S, Manickam S, Velayutham R, Natesan S. Improved Topical Drug Delivery: Role of Permeation Enhancers and Advanced Approaches. Pharmaceutics. 2022. doi:10.3390/pharmaceutics14122818

47. Opatha SAT, Titapiwatanakun V, Chutoprapat R. Transfersomes: A promising nanoencapsulation technique for transdermal drug delivery. Pharmaceutics. 2020. p. 1–23. doi:10.3390/pharmaceutics12090855
48. Nayak D, Tippavajhala VK. A comprehensive review on preparation, evaluation and applications of deformable liposomes. Iran J Pharm Res. 2021. p. 186–205. doi:10.22037/ijpr.2020.112878.13997
49. Almeida Junior S de. In vivo methods for the evaluation of anti-inflammatory and antinoceptive potential. Brazilian Journal Of Pain. 2019;2(4). doi:10.5935/2595-0118.20190070
50. Mcnamara CR, Mandel-Brehm J, Bautista DM, Siemens J, Deranian KL, Zhao M, et al. TRPA1 mediates formalin-induced pain. PNAS August [Internet]. 2007. Available from: www.pnas.org/cgi/content/full/0705924104/DC1.www.pnas.orgcgidoi10.1073pnas.0705924104
51. Masocha W, Kombian SB, Edafiogho IO. Evaluation of the antinociceptive activities of enaminone compounds on the formalin and hot plate tests in mice. Sci Rep. 2016 Feb 26;6. doi:10.1038/srep21582 PubMed PMID: 26916642.
52. Yashpal K, Codertea TJ. Influence.of formalin concentration on the antinociceptive effects of anti-inflammatory drugs in the formalin test in rats: separate mechanisms underlying the nociceptive effects of low-and high-concentration formalin. European Journal of Pain. 1998.
53. Sallam MA, Motawaa AM, Mortada SM. A modern approach for controlled transdermal delivery of diflunisal: Optimization and in vivo evaluation. Drug Dev Ind Pharm. 2013;39(4):600–10. doi:10.3109/03639045.2012.692476 PubMed PMID: 22697341.
54. Croffod LJ. Use of NSAIDs in treating patients with arthritis. Arthritis Res Ther. 2014;15.
55. Madhavi N, Sudhakar B, Suresh Reddy KVN, Vijaya Ratna J. Pharmacokinetic and pharmacodynamic studies of etodolac loaded vesicular gels on rats by transdermal delivery. DARU, Journal of Pharmaceutical Sciences. 2018 Sep 1;26(1):43–56. doi:10.1007/s40199-018-0214-4
56. Siriwardane DA, Wang C, Jiang W, Mudalige T. Quantification of phospholipid degradation products in liposomal pharmaceutical formulations by ultra performance liquid chromatography-mass spectrometry (UPLC-MS). Int J Pharm. 2020 Mar 30;578. doi:10.1016/j.ijpharm.2020.119077 PubMed PMID: 31988036.
57. Maslii Y, Ruban O, Kasparaviciene G, Kalveniene Z, Materiienko A, Ivanauskas L, et al. The Influence of pH Values on the Rheological, Textural and Release Properties of Carbomer Polacril® 40P-Based Dental Gel Formulation with Plant-Derived and Synthetic Active Components. Molecules. 2020 Oct 29;25(21). doi:10.3390/molecules25215018 PubMed PMID: 33138200.
58. Song F, Yang G, Wang Y, Tian S. Effect of phospholipids on membrane characteristics and storage stability of liposomes. Innovative Food Science & Emerging Technologies. 2022;81:103155. doi:10.1016/j.ifset.2022.103155